NUCL SCI TECH (2019) 30:45
https://doi.org/10.1007/s41365-019-0567-5

Method for the determination of polonium-210 in tea samples using response surface methodology (RSM)

Sermin Çam Kaynar[1] · **Ümit H. Kaynar**[2]

Received: 24 May 2018 / Revised: 13 July 2018 / Accepted: 20 July 2018 / Published online: 13 February 2019

Abstract The method based on solvent parameters (mass, cycle of acidification, and autodeposition time), combined with response surface methodology (RSM) modeling and optimization, has been developed for maximizing ^{210}Po activity in tea samples, as observed by an alpha spectrometer. RSM based on 3-factor and 5-level composite center design was used to obtain the optimal combination of solvent conditions. As solvent parameters for ^{210}Po activity, different masses (0.5, 0.75, 1, 1.5, and 2 g), different cycles of acidification (2, 3, 4, 5, and 6 times), and different autodeposition times (2, 3, 4, 5, and 6 h) were studied. The 3D response surface plot and the contour plot derived from the mathematical models were used to determine the optimal conditions. According to the obtained results, the experimental value of ^{210}Po activity was in good agreement (R^2=0.96) with the value predicted by the model. We found a favorable effect of mass on the ^{210}Po activity ($p<0.05$).

Keywords ^{210}Po activity · Tea · Response surface methodology

1 Introduction

Environmental radiation arises from various naturally occurring and man-made sources [1]. The largest contribution to radiation exposure comes from natural sources (approximately 86%), while man-made sources contribute only 14%. Doses from other man-made or artificial sources account for less than 1% [2, 3]. Among natural radionuclides, ^{210}Po ($T_{1/2}$, 138.4 d) from the ^{238}U series is significant due to its potential internal human radiation exposure. It is an alpha emitter with high linear energy transfer and exists in trace amounts in most plants and foodstuffs [4, 5]. It is among the most radiotoxic nuclides to humans [4] and may be a cause of lung cancer [6].

Tea is one of the most widely consumed beverages in the world. It is consumed daily by many countries and is prepared from the *Camellia sinensis* leaves. Tea leaves are usually characterized by the increased contents of radionuclide contaminants like ^{210}Pb, ^{210}Bi, and ^{210}Po [7] because of the deposition of aerosols containing these radionuclides on tea leaves. There have been several studies related to radionuclides on various teas [2, 7–13]. Determination of the activity concentrations of radionuclides (primarily ^{210}Po) in tea remains important; therefore, we chose to determine ^{210}Po in tea samples.

This study was aimed to determine the optimum solvent parameters for the activity of ^{210}Po in tea samples using response surface methodology (RSM). The mass of the sample, cycle of acidification, and autodeposition time were analyzed using a central composed design (CCD).

✉ Sermin Çam Kaynar
sermin.cam@cbu.edu.tr

[1] Physics Department, Faculty of Science and Letters, Manisa Celal Bayar University, 45140 Manisa, Turkey

[2] Science Education, Faculty of Education, Manisa Celal Bayar University, Manisa, Turkey

2 Material and method

2.1 Experimental process

Tea samples were dried to constant weight at room temperature. Different masses (0.5, 0.75, 1, 1.5, and 2 g) were weighed and added to a 250-mL beaker. The concentrated acids (3 mL 65% HNO_3+5 mL 35% H_2O_2) were added to the sample, and the beaker was covered with a watch glass and allowed to stand overnight at room temperature. Then, the solution was heated on a hot plate at 95 °C and evaporated to near dryness. Then, mixed acids (3 mL HNO_3 and 9 mL 37% HCl) were added to the precipitate followed by re-heating on the hot plate (at 95 °C) and evaporation to near dryness. The acidification process was repeated 2–6 times. After evaporation, 200 mL of 0.5 M HCl was added to the precipitate and filtered through a filter paper (particle retention 10–15 µm, 125 mm diameter, 84 g m^{-2} weight) into a 250-mL beaker. Ascorbic acid (0.5 g) was added to the beaker to reduce Fe^{3+} concentration.

Copper disks of diameter 2.5 cm were cut from a copper plate. They were first wiped with acetone and then left in 1 M HNO_3 for 1–2 m, washed with pure water, and dried at room temperature. The dried copper disks were placed inside a bottle cap with the front face cut out and were compressed with a magnetic bar to prevent it from falling. The prepared copper disks were placed in a 200 mL sample solution so that the magnetic bar portion was below. The autodeposition process was performed on a hot plate. ^{210}Po was spontaneously accumulated on the copper disk at the 70 °C (Fig. 1).

The activity of ^{210}Po was determined by using an alpha spectrometer equipped with a 450-20 AM PIPS detector. The energy resolution was ≤20 keV, the detector efficiency was ≥25%, and the background was ≤1 count per hour above 3 MeV. System calibration was done by using a ^{241}Am point source. The ^{210}Po activity concentration of the samples collected onto the copper disk was counted by using the alpha spectrometer based on the alpha-particle emission peak with 5.30 MeV energy, and ^{209}Po as the internal tracer. The ^{210}Po activity concentration was calculated at different autodeposition times on the copper disk. The chemical efficiency was 37.7% for ^{209}Po. The ^{210}Po activity concentration for each sample was corrected for the recovery using the total efficiency.

2.2 Response surface methodology (RSM)

RSM is an effective method to solve multivariable problems and provides optimization of many dependent variables in various experiments. It involves mathematical and statistical techniques used to determine the optimum operating conditions in a given system or to determine how it is affected by the independent variables of one or more dependent variables in a region of interest [14–17]. Independent variables (X_1: sample mass, X_2: cycle of acidification, and X_3: autodeposition time) were examined on five levels. These variables and their coded levels of CCD design are given in Table 1.

The regression model equation was given as follows:

$$Y = b_0 + \sum_{i=1}^{2} b_i x_i + \sum_{i=1}^{2} b_{ii} x_i^2 + \sum_{i=1}^{1} \sum_{j=i+1}^{2} b_{ii} x_i x_j + \varepsilon, \qquad (1)$$

where Y is the response, b_0 is the intercept, b_{ij}, b_{ii}, and b_i

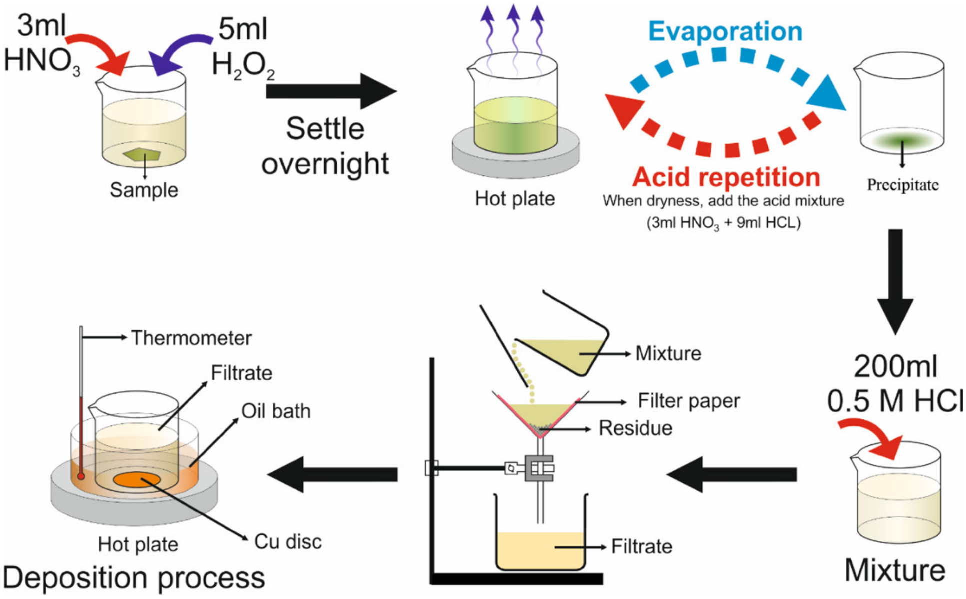

Fig. 1 (Color online) Flow diagram of the entire process

Table 1 Independent variables and their coded levels used for optimization

Factors	Factor code	Range and levels (coded)				
		−1.6818	−1	0	1	1.6818
Mass (g)	X_1	0.5	0.75	1	1.5	2
Cycle of acidification (times)	X_2	2	3	4	5	6
Autodeposition time (h)	X_3	2	3	4	5	6

are the coefficients, n is the number of variables, x_i and x_j are the independent variables, and ε is the error. The optimum data of the chosen variable were found using RSM plots and the regression equation. The correlation coefficient (R^2) was found to be high (0.96). The significance of the RSM model was evaluated for the probability value (Prob>F) and F value. For this calculation, the second-order polynomial equation was as follows:

$$Y = b_0 + b_1X_1 + b_2X_2 + b_3X_3 + b_{11}X_1^2 + b_{22}X_2^2 + b_{33}X_3^2 + b_{12}X_1X_2 + b_{13}X_1X_3 + b_{23}X_2X_3 \quad (2)$$

The experiments were performed under optimum conditions obtained by RSM (Table 2). Initial studies were conducted to determine the required mass (X_1: 0.5, 0.75, 1, 1.5, and 2 g), the cycle of acidification (X_2: 2, 3, 4, 5 and 6 times), and autodeposition time (X_3: 2, 3, 4, 5, and 6 h). The total design consisted of 20 experimental points. The matrix of the design is listed in Table 2, and six replicates (runs 15–20) were performed at the center of the design.

Excel and Minitab 17 were used for graphical analysis and regression analysis of the acquired data. Analysis of variance (ANOVA) was done to obtain the probability and F value. In addition, the statistical parameters were calculated with RSM; the optimum values were found from the regression equation and the RSM surface/counter plots.

3 Results and discussion

The second-order polynomial equation was obtained by CCD design for elucidating the relationship between the ^{210}Po activity and the three independent variables. According to the obtained results, quadratic model equality, given the activity of ^{210}Po, was as follows:

Table 2 Experimental design values for tea

Run order	X_1	X_2	X_3	Mass (g)	Cycle of acidification (HNO_3/HCl, 3:9)	Autodeposition time (h)	^{210}Po activity (Bq)	
							Experimental	Predicted
1	−1	−1	−1	0.75	3	3	0.049	0.049
2	−1	−1	1	0.75	3	5	0.042	0.038
3	−1	1	−1	0.75	5	3	0.050	0.042
4	−1	1	1	0.75	5	5	0.043	0.044
5	1	−1	−1	1.5	3	3	0.103	0.100
6	1	−1	1	1.5	3	5	0.088	0.095
7	1	1	−1	1.5	5	3	0.089	0.091
8	1	1	1	1.5	5	5	0.100	0.099
9	−1.6818	0	0	0.5	4	4	0.026	0.032
10	1.6818	0	0	2	4	4	0.126	0.122
11	0	−1.6818	0	1	2	4	0.071	0.070
12	0	1.6818	0	1	6	4	0.065	0.068
13	0	0	−1.6818	1	4	2	0.060	0.065
14	0	0	1.6818	1	4	6	0.066	0.063
15	0	0	0	1	4	4	0.072	0.069
16	0	0	0	1	4	4	0.076	0.069
17	0	0	0	1	4	4	0.06	0.069
18	0	0	0	1	4	4	0.069	0.069
19	0	0	0	1	4	4	0.069	0.069
20	0	0	0	1	4	4	0.069	0.069

Table 3 Analysis of variance of the regression model for ^{210}Po activity

ANOVA	*df*	SS	MS	*F*	Probability *F*
Regression	9	0.009996828	0.001111	28.79688	0.00000542
Residual	10	0.000385722	0.0000386		
Total	19	0.01038255			

Multiple R^2=0.96, adjusted R^2=0.93

Table 4 Estimated regression coefficients and the *F* and *p* values

Regression	Coefficients	Standard error	*F*	*p*
Intercept	0.069118	0.002533004	27.28693	1.01 E−10*
X_1	0.026666	0.001680587	15.86729	2.03 E−08*
X_2	−0.00074	0.001680587	−0.43966	0.669536
X_3	−0.00058	0.001680587	−0.3446	0.73753
X_1X_1	0.002735	0.001635999	1.671513	0.125571
X_2X_2	−0.000094	0.001635999	−0.05734	0.955403
X_3X_3	−0.00186	0.001635999	−1.13788	0.2817
X_1X_2	−0.0005	0.002195797	−0.22771	0.824462
X_1X_3	0.00125	0.002195797	0.569269	0.581734
X_2X_3	0.00325	0.002195797	1.480101	0.169648

*Significant (p<0.05)

$$\begin{aligned} Y = {} & 0.069 + 0.027\ \text{Mass (g)} \\ & - 0.0007\ \text{Cycle of acidification} \\ & - 0.0006\ \text{Autodeposition time (h)} \\ & + 0.003\ \text{Mass (g)} \times \text{Mass (g)} \\ & - 0.000094\ \text{Cycle of acidification} \\ & \times \text{Cycle of acidification} \\ & - 0.002\ \text{Autodeposition time (h)} \\ & \times \text{Autodeposition time (h)} - 0.0005\ \text{Mass (g)} \\ & \times \text{Cycle of acidification} + 0.0013\ \text{Mass (g)} \\ & \times \text{Autodeposition time (h)} \\ & + 0.0033\ \text{Cycle of acidification} \\ & \times \text{Autodeposition time (h)}. \end{aligned} \tag{3}$$

The synergistic and antagonistic influences were described with positive and negative parameters, respectively. For obtaining the statistical explanation of the above equation with *t* test, second-order variance analysis of the response surface (ANOVA) was performed (Table 3). Since the obtained *F* value was 28.79688, the experimental yields obtained by changing the factor levels were statistically meaningful at the 95% confidence limit. According to the results, the model was compatible where the smaller *p* values (<0.0001) indicated that the model was significant. R^2 of the second-order model calculated for the ^{210}Po activity (Bq) was very close to 1 (0.96), implying that the experimental data agreed with the values predicted by the

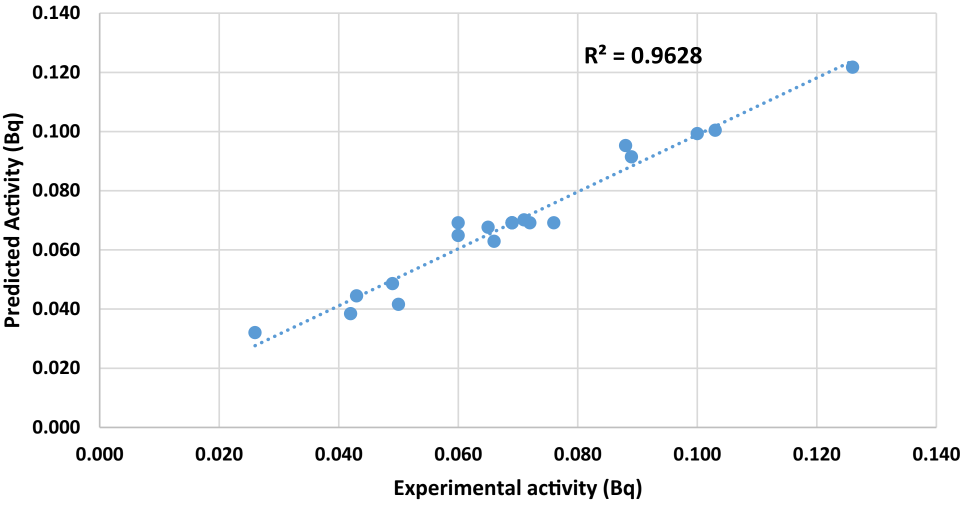

Fig. 2 Correlation of experimental and predicted activity of ^{210}Po

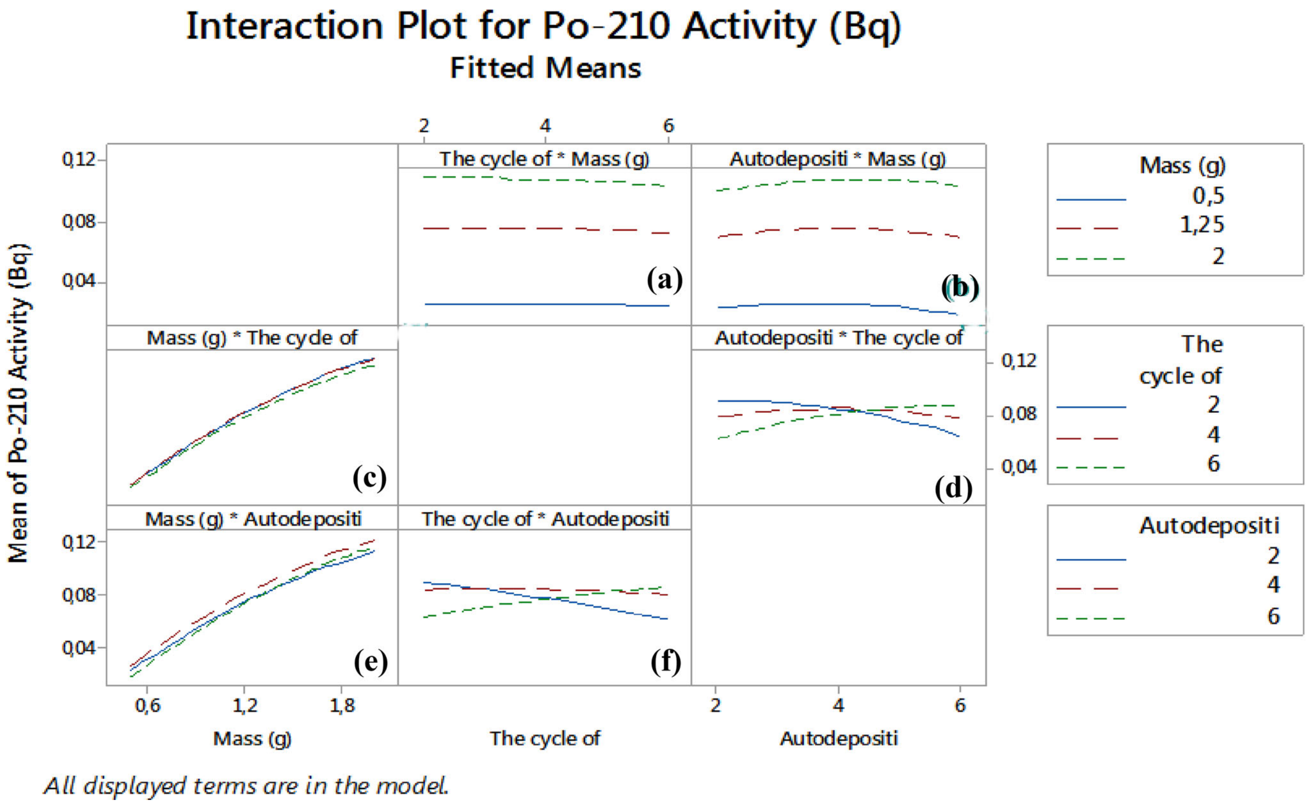

Fig. 3 (Color online) Interaction plots for ^{210}Po activity. (a) Cycle of acidification and mass, (b) autodeposition time and mass, (c) mass and cycle of acidification, (d) autodeposition time and cycle of acidification, (e) mass and autodeposition time, (f) cycle of acidification and autodeposition time

Fig. 4 Main effects plot for ^{210}Po activity (Bq)

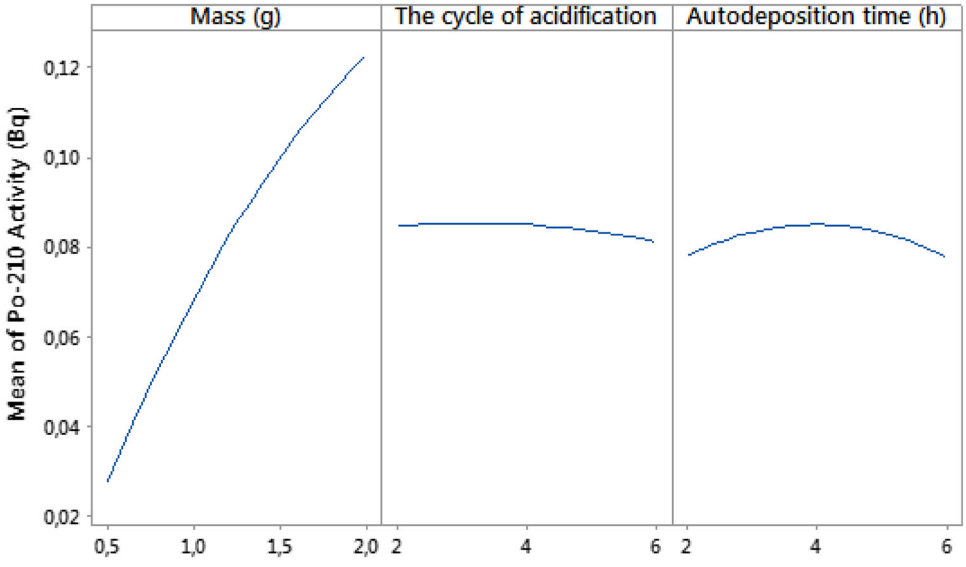

model. The adjusted determination coefficient (Adj. R^2= 0.93) was also close to 1.

The significance of each coefficient is given in Table 4, with an F value and a p value. The larger the F values and the smaller the p values, the more significant are the corresponding coefficients. The regression was statistically significant at p values less than 0.05 and 0.01, as shown in Table 4. Thus, ^{210}Po activity was affected significantly by

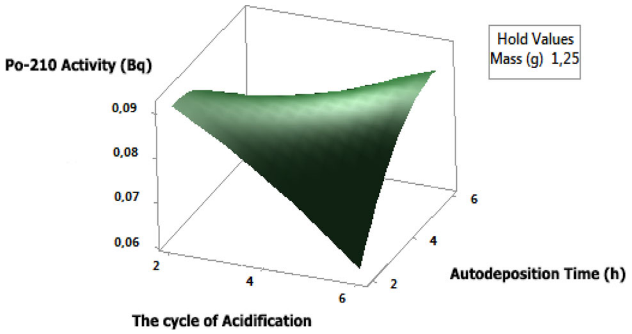

Fig. 5 (Color online) Response surface graphs for interactions between investigating parameters (acidification and autodeposition time) of ^{210}Po activity

the parameters (X_1, X_1X_1, X_1X_3, and X_2X_3 ($p<0.05$); the quadratic parameters (X_2, X_{11}, X_{22}, and X_{12}) were insignificant ($p>0.05$).

The plot of the predicted activity against the experimental ^{210}Po activity is shown in Fig. 2. The experimental activity values were distributed close to the straight line. This showed that the predicted values of the model were in good agreement with the experimental values. This is an evidence of the validity of the regression model. The regression coefficient calculated for the model was R^2= 0.96, and it showed the agreement of the values obtained from the model with real values. ^{210}Po activity values obtained in this study for different cycles of acidification and different masses were positive.

Interaction plots for ^{210}Po activity are shown in Figs. 3 and 4. ^{210}Po activity (Bq) increased upon increasing the sample mass from 0.5 to 2 g as shown in Figs. 3c, d and 4. With variations in sample mass, cycle of acidification, and autodeposition time, ^{210}Po activity changed as follows: ^{210}Po activity increased with increasing sample mass

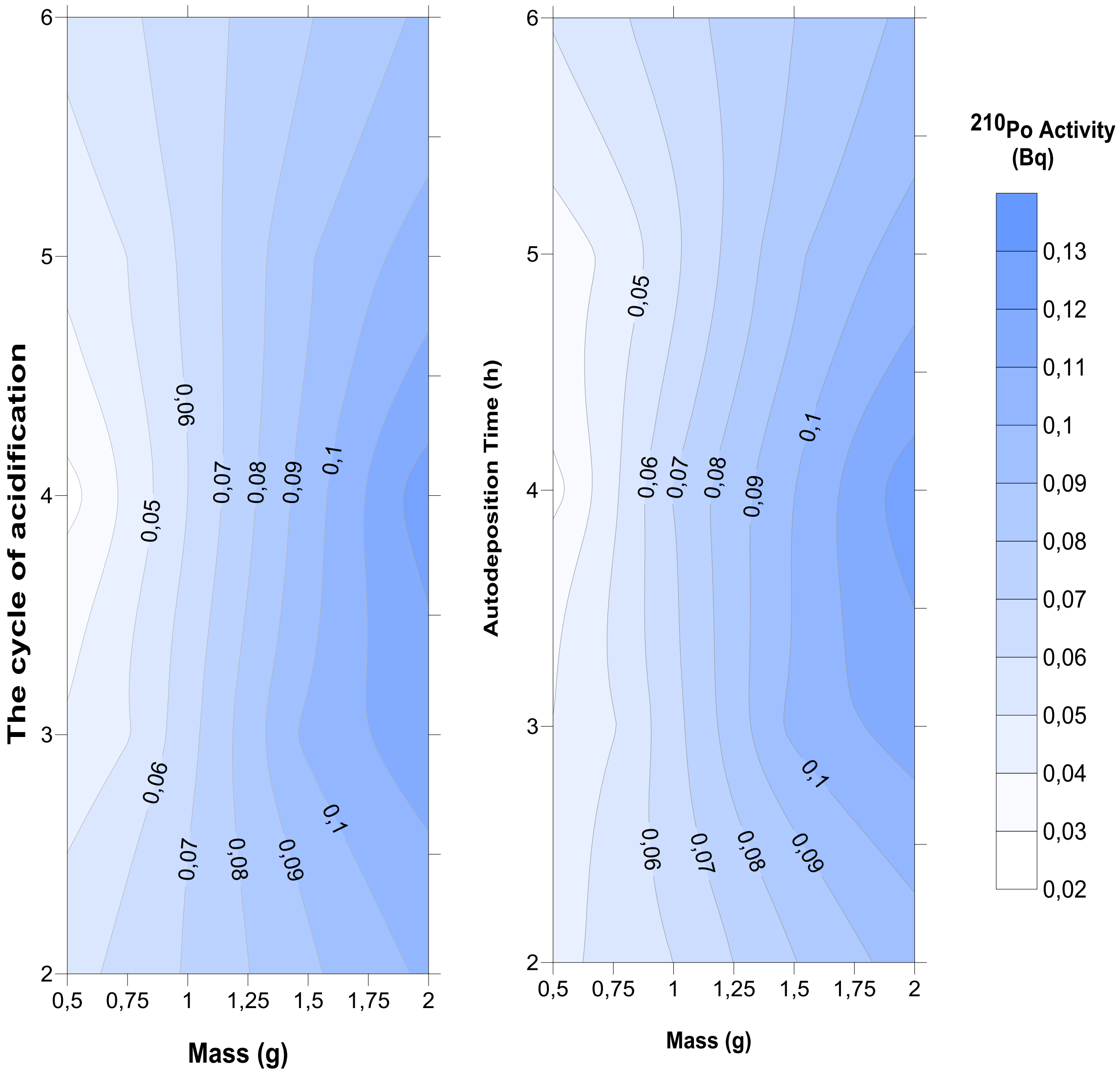

Fig. 6 (Color online) Contour color map graphs for the interaction of investigation parameters of ^{210}Po activity

(Fig. 3c, e) and remained constant for different cycles of acidification and autodeposition times (Fig. 3a, b). Figure 3d shows that with increasing autodeposition time, the ^{210}Po activity decreased for 2 cycles of acidification (blue line), remained unchanged for 4 cycles of acidification (red line), and increased for 6 cycles of acidification (green line). In Fig. 3d, f, the point of intersection of the lines for the cycle of acidification and autodeposition time is 4. In other words, 4 cycles of acidification and 4 h of autodeposition time were found to be optimal for the activity.

The combined effect of cycle of acidification and autodeposition time (h) is shown in Fig. 5. The maximum activity of ^{210}Po was determined to be 0.87 Bq at a sample mass of 1.25 g.

Contour color map graphs of ^{210}Po activity (Fig. 6) showed the effects of the interactions between mass (X_1) and cycle of acidification (X_2) as well as that between mass (X_1) and autodeposition time (X_3) on the ^{210}Po activity. An increase in mass from 0.5 to 2 g improved the activity yield. In addition, increasing the cycle of acidification and autodeposition time leads to a reduction in ^{210}Po activity. When more than 4 cycles of acidification were performed and the autodeposition time was more than 4 h, there was a reduction in activity. The maximum activity was obtained for 4 cycles of acidification and autodeposition time of 4 h. Thus, for the maximum activity result of the tea samples, optimal conditions were as follows: 1 g of the sample mass, 4 cycles of acidification, and 4 h of autodeposition time.

4 Conclusion

In this study, RSM was used to model and optimize the conditions for maximum ^{210}Po activity in tea samples. The effect of three independent variables (sample mass, cycle of acidification, and autodeposition time) on ^{210}Po activity was obtained by using RSM surface plot and contour plots. The optimal conditions for maximum ^{210}Po activity in tea samples were as follows: sample mass of 1 g, 4 cycles of acidification, and autodeposition time of 4 h. The experimental activity values and the predicted activity values of ^{210}Po agree with each other. In brief, this study provides a new efficient method for the determination of ^{210}Po activity in tea sample.

References

1. F.K. Görür, R. Keser, N. Akçay et al., Annual effective dose and concentration levels of gross α and β in Turkish market tea. Int. J. Radiat. Res. **10**, 67–72 (2012)
2. M.G. Shooshtari, M.R. Deevband, M.R. Kardan et al., Analytical study of Ra-226 activity concentration in market consuming foodstuffs of Ramsar, Iran. J. Environ Health Sci. Eng. **15**, 1–7 (2017). https://doi.org/10.1186/s40201-017-0281-3
3. Environmental Protection Agengy (EPA) (2018), http://www.epa.ie/radiation/radexp. Accessed 16 Feb 2018
4. A.E.M. Khater, Polonium-210 budget in cigarettes. J. Environ. Radioact. **71**, 33–41 (2004). https://doi.org/10.1016/S0265-931X(03)00118-8
5. N.S. Fisher, K.B. Seiller, T.G. Hinton et al., Evaluation of radiation doses and associated risk from the Fukushima nuclear accident to marine biota and human consumers of seafood. Proc. Natl. Acad. Sci. USA **110**, 10670–10675 (2013). https://doi.org/10.1073/pnas.1221834110
6. M. Horvath, A. Shahrokhi, P. Bator et al., Determination of Po-210 content in cigarette smoke using a smoking machine: A case study of Iranian cigarettes. J. Environ. Radioact. **174**, 66–70 (2017). https://doi.org/10.1016/j.jenvrad.2017.01.023
7. E.V. Puchkovaa, O.G. Bogdanova, ^{210}Po in black and green teas. Radiochemistry **58**, 98–105 (2016)
8. M.S. Al-Masri, A. Nashawati, Y. Amin et al., Determination of ^{210}Po in tea, mate and their infusions and its annual intake by Syrians. J. Radioanal. Nucl. Chem. **260**, 27–34 (2004)
9. F.K. Görür, R. Keser, N. Akçay et al., Radionuclides and heavy metals concentrations in Turkish market tea. Food Control **22**, 2065–2070 (2011). https://doi.org/10.1016/j.foodcont.2011.06.005
10. D. Desideri, M.A. Meli, C. Roselli et al., Alpha and gamma spectrometry for determination of natural and artificial radionuclides in tea, herbal tea and camomile marketed in Italy. Microchem. J. **98**, 170–175 (2011). https://doi.org/10.1016/j.microc.2011.01.005
11. D.E. Di Gregorio, H. Huck, R. Aaristegui et al., ^{137}Cs contamination in tea and yerba mate in South America. J. Environ. Radioact. **76**, 273–281 (2004). https://doi.org/10.1016/j.jenvrad.2003.11.008
12. M.C. Cook, M.J. Stukel, W. Zhang et al., The determination of Fukushima-derived cesium-134 and cesium-137 in Japanese green tea samples and their distribution subsequent to simulated beverage preparation. J. Environ. Radioact. **153**, 23–30 (2016). https://doi.org/10.1016/j.jenvrad.2015.12.010
13. N. Fathabadi, A.A. Salehi, K. Naddafi et al., Radioactivity levels in the mostly local foodstuff consumed by residents of the high level natural radiation areas of Ramsar, Iran. J. Environ. Radioact. **169–170**, 209–213 (2017). https://doi.org/10.1016/j.jenvrad.2016.12.011
14. S.F. Mutlu, İki basamaklı tepkime ile sıvı özütlemeli yöntem kullanarak fındık tohum kabuklarından furfural üretimi için en uygun koşulların istatistik yöntem ile belirlenmesi. J. Fac. Eng. Archit. Gazi Univ. **25**, 21–26 (2010). **(in Turkish)**
15. L.C. Zhao, Y. He, X. Deng et al., Response surface modeling and optimization of accelerated solvent extraction of four lignans from fructus schisandrae. Molecules **17**, 3618–3629 (2012). https://doi.org/10.3390/molecules17043618
16. S. Sharma, A. Malik, S. Satya, Application of response surface methodology (RSM) for optimization of nutrient supplementation for Cr(VI) removal by *Aspergillus lentulus* AML05. J. Hazard. Mater. **164**, 1198 (2009). https://doi.org/10.1016/j.jhazmat.2008.09.030
17. A. Dean, D. Voss, D.D. Draguljic, *Response Surface Methodology, Design and Analysis of Experiments* (Springer, New York, 2017). ISBN 978-3-319-52250-0